



PREDICTIVE STUDY OF LAMINAR NATURAL CONVECTION IN SUPERCRITICAL FLUID ALONG VERTICAL FLAT PLATE

*Dr. Adil Abbas Mohammed¹, Saad Abdulwahab Razuqi²

1) Lecturer, Mechanical Engineering Department, Al-Mustansiriyah University, Baghdad, Iraq.

2) Asst. Lecturer., Mechanical Engineering Department, Al-Mustansiriyah University, Baghdad, Iraq.

Abstract: The laminar natural convection in supercritical fluid along vertical flat plate with uniform heat flux was simulated in the present work. The governing equations of partial differential equations were solved numerically using the finite difference method. The thermo-physical properties calculation was based on a Van der Waals equation of state. The velocity and temperature profiles were solved with a FORTRAN code. Hydrofluorocarbons R134a, R1234yf and R404a were used as working fluids. Thermal expansivity at a reduced pressure and reduced temperature near critical point (Pr and $Tr = 1.05, 1.1$) showed sharp variation. The local Nusselt number as a function of the local Rayleigh number was plotted. The curve trend illustrates that the Nusselt number decreases as the reduced pressure and reduced temperature increases. The corresponding curves of supercritical conditions depict the same shape of the corresponding line of classic correlation. The velocity and temperature developing along the vertical plate was plotted and contour lines explained the fluid behavior above supercritical conditions.

Keywords: *Supercritical; convection; refrigerant; flat plate; laminar; Numerical Analysis.*

دراسة تنبؤية عن الحمل الطبيعي الطبقي داخل مائع فوق الحرج على صفيحة عمودية

الخلاصة: يتضمن العمل الحالي اجراء محاكاة للحمل الطبيعي للسوائل فوق النقطة الحرجة على طول لوحة مسطحة عمودية بوجود فيض حراري ثابت. تم حل المعادلات التي تحكم المعادلات التفاضلية الجزئية عدديا باستخدام طريقة الفروق المحدودة. تم احتساب الخصائص الفيزيائية الحرارية حسب المعادلة العامة للغازات الخاصة بفان دير فال. تم حل اشكال السرعة ودرجة الحرارة باستخدام برنامج FORTRAN. استخدمت المركبات الكربونية الفلورية الهيدروجينية R134a، و R1234yf و R404a كموائع للعمل. أظهر معامل التمدد الحجمي لقيم معامل انخفاض الضغط ودرجة الحرارة بالقرب من النقطة الحرجة (Pr and $Tr = 1.05, 1.1$) انحراف الحاد. تم رسم العلاقة بين رقم نسلت ورقم ريلي. المنحنيات المقابلة للظروف فوق الحرجة تصور نفس الشكل من خط المقابلة من الارتباط الكلاسيكي. تم رسم سرعة ودرجة الحرارة النامية على طول لوحة عمودية وخطوط التطور تشرح سلوك السوائل في الظروف فوق الحرجة.

1. Introduction

The natural convection along a vertical flat plate is an important phenomenon and are widely seen in engineering applications in electronic cooling equipment, building with most of the formatting specifications needed for preparing their papers. Margins, line spacing, and type styles are built-in; examples of the type styles are provided throughout this document, application, crystal growth progresses, geothermal reservoirs,

petroleum industries, transpiration cooling, storage of radioactive nuclear waste materials, separation processes in chemical industries, building thermal insulation, and solar heating systems. All these applications were extensively studied in the recent years. The water represents the main fluid in the above mentioned applications [1].

The region close to the critical point where the property variations are severe and the heat transfer effects change spontaneously. They are generally largest when the temperatures of the hotter surface and the fluid span the critical temperature, for example, that the compressibility and the specific heat at constant pressure both become infinite at the critical point. These factors make experimentation difficult, the hydrostatic pressure variation in the fluid will lead to significant density variations even for small changes of height and the approach to thermal equilibrium will be slow as specific heat becomes large. Regarding the working fluid selection, the growing attention to environmental impact limits the number of fluids under investigation as ideal candidates should exhibit a low ozone depleting potential (ODP) and low global warming potential (GWP) [2].

Several conventional refrigerants including R134a, R1234yf, and R404a have been proposed as working fluids for the supercritical cycles with various performance characteristics. R134a has been widely used as a refrigerant for domestic refrigerators and automobile air conditioners. R134a is more suitable as the working fluid in supercritical cycles for high-temperature heat generation because of its higher critical temperature and lower operating pressure, as well as its fairly good thermos-physical properties and good thermal stability. Supercritical cycles with R134a as the working fluid for geothermal power generation system has been proposed and studied. When the R134a is above the critical pressure ($P_{cr} = 4059$ kPa, $T_{cr} = 101$ °C), as shown in figure 1. For R134a, a corollary of its high critical temperature is its low volumetric capacity. The thermos-physical characteristics specific heat, density, thermal conductivity and viscosity will be strongly influenced and quite different from those of fluids with constant thermos-physical properties [3].

R1234yf with critical pressure, ($P_{cr} = 3382$ kPa, $T_c = 94.7$ °C), as shown in figure 2, has smaller latent heat of vaporization which leads to larger mass flow rates, larger pressure drops in heat exchangers and connection pipes, and ultimately, lower coefficients of performance. R1234yf has low toxicity, similar to R134a, and mild flammability [4]. R404a is ozone-friendly in a window air-conditioner, has a low critical temperature and pressure 72.12°C and 3735 kPa, respectively as shown in figure 3. To achieve the desired heat rejection temperatures for these applications, refrigerant blends such as R404A has low critical temperature and high molar heat capacity must either operate as condensers at pressures close to their critical pressure, or as gas coolers exceeding the critical pressure [5].

Many experimental and numerical studies of rectangular flat plates have been carried. The enhancement of natural convection heat transfer has received significant attention because it happened in different fields of engineering such as heat exchangers and refrigeration industries, cooling techniques for electronic components, geothermal systems, thermal insulation for buildings, solar collectors and space heating, and the solution of the effect of exponential and power law

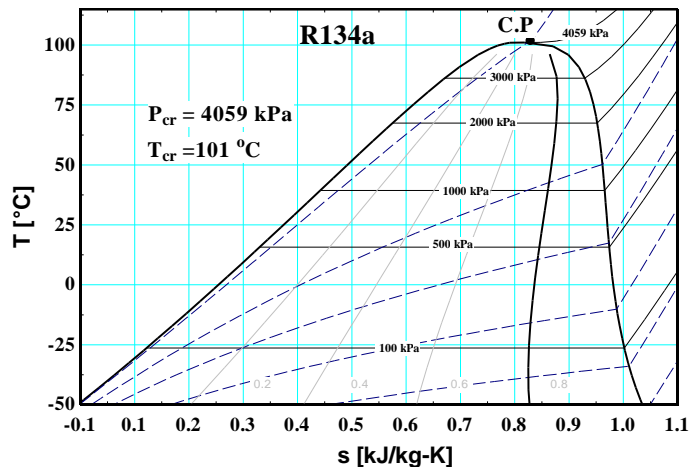


Figure 1. Physical properties of R134a at supercritical pressures.

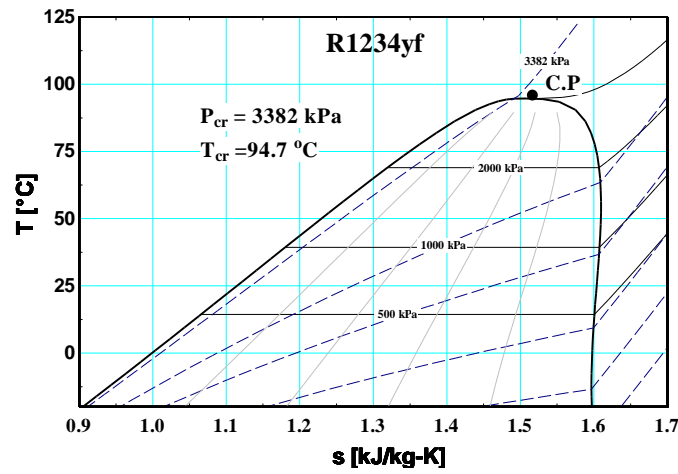


Figure 2. Physical properties of R1234yf at supercritical pressures.

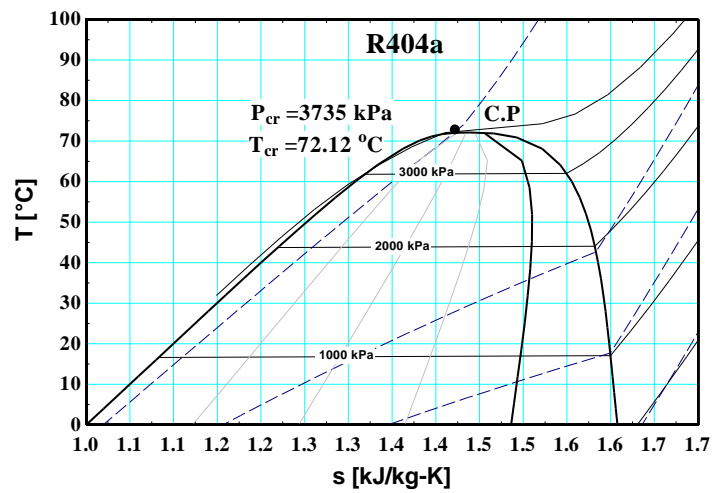


Figure 3. Physical properties of R404a at supercritical pressures.

temperature distributions on heat transfer Convection along non-isothermal vertical flat plate has been presented [6].

Ostrach,(1952) [7] was one of the first to solve the set of equations (continuity, momentum and energy) with numerical method for the boundary layer and natural convection along vertical flat plate reducing the set of three equations with the respective boundary conditions. He concluded that the flow is affected by the Grashof number and Prandtl number. Supercritical fluids is one of the most promising methods for heat transfer performance of base fluids heated to above the critical temperature and compressed to above the critical pressure is known as a supercritical fluid. Supercritical fluids can be applied in many fields such as drug delivery, chromatography, synthesis, purification and extraction. Above the critical point of a fluid, the changes in pressure or temperature significantly alters the physico-chemical properties of the supercritical fluid (density, diffusivity) especially important for synthetic applications [8].

2. Mathematical Model

The mathematical approach describing natural convection for simple geometries by using the energy equation and the Navier-Stokes equations are first stated and simplified for the particular geometry being studied. Then, the density of the fluid is expressed in terms of the thermal expansivity, (assumed constant) and the temperature and substituted into the Navier-Stokes equations. The variable physical properties of the fluid was taken into account. In many applications, convection heat transfer is coupled with conduction and radiation heat transfer, which generate temperature gradients along the walls and may greatly affect natural convection heat transfer.

The influence of the non uniformity of wall temperature on the heat transfer by natural convection from a non-isothermal vertical plate into a supercritical fluid [9]. The thermal expansion coefficient is considered as a function of the temperature, the pressure, the van der Waals constants and the compressibility factor (Z).

The trends of the curves obtained with this equation and with values from tables of thermodynamic properties were similar and diverged at a critical point. These features conformed the validity of this equation. Then, the governing systems of partial differential equations are solved numerically using the finite difference method. The local Nusselt number was then calculated and plotted as a function of the local Rayleigh number. It was observed that a positive slope of temperature distribution increases the heat transfer rate and a negative slope decreases it.

2.1. Boussinesq approximation and governing equations

For the laminar vertical plate case a need for the laminar boundary layer equations to be incorporated with natural convection which is based on the assumptions of a steady, incompressible, two dimensional flow, with constant fluid properties and the Boussinesq approximation. In addition it is commonly assumed, that the velocity normal to the boundary is small, and derivations in direction of the flow are negligible. Natural convection is observed when density gradients are present in a fluid acted upon

by a gravitational field. Flow and heat transfer are analyzed by using the continuity, momentum and energy balance equations that govern these processes. Free convection refers to fluid motion induced by buoyancy forces. The Buoyancy forces may arise in a fluid for which there are density gradients, and a body force that is proportional to density. In heat transfer, density gradients are due to temperature gradients and the body force is gravitational. The governing equations to satisfy this model are defined as a dimensionless variables:

2.1.1. Continuity equation.

$$\frac{D\rho}{\rho Dt} + \nabla \cdot \mathbf{U} = 0 \quad (1)$$

By Boussinesq approximation:-

$$\nabla \cdot \mathbf{U} = 0 \quad (2)$$

$$\frac{\partial U}{\partial X} + \frac{\partial V}{\partial Y} = 0 \quad (3)$$

2.1.2. Momentum Equation.

$$\left(U \frac{\partial U}{\partial X} + V \frac{\partial U}{\partial Y} \right) = \theta \beta^* + \frac{\partial^2 U}{\partial Y^2} \quad (4)$$

Where $\beta^* = \frac{\beta}{\beta_{ref}}$

2.1.3. Energy Equation.

$$U \frac{\partial \theta}{\partial x} + V \frac{\partial \theta}{\partial y} = \left(\frac{1}{Pr} \right) \left(\frac{\partial^2 \theta}{\partial Y^2} \right) \quad (5)$$

Where $X = \frac{x}{LG^o}$, $Y = \frac{y}{W}$, $\theta = \frac{T-T_\infty}{T_s-T_\infty}$

$$U = \frac{uW^2}{vLGr}, \quad V = \frac{vW}{\gamma}, \quad Gr = \frac{\beta_{ref} g(T_s-T_\infty)W^4}{\gamma^2 L} \quad (7)$$

2.2. Finite-Difference Equations

To express the set of dimensionless partial differential equations in finite-difference form, the grid system is used, with i-lines running in the Y-direction normal to the surface and j-lines running in the X-direction parallel to the surface. The equations of motion, of energy, and continuity are now discretized based on such notation as shown in figure .4.

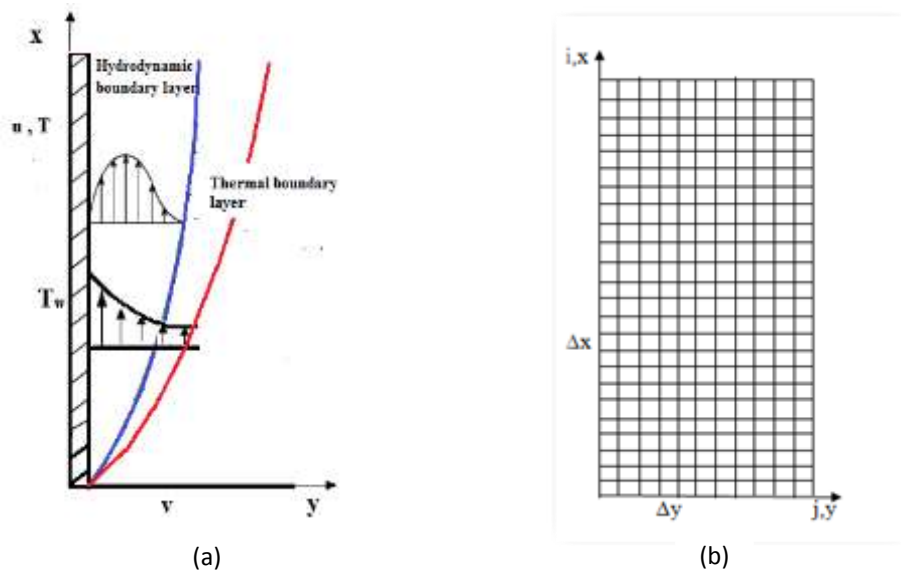


Figure 4. (a) Modeling description, (b) Grid used in the numerical solution

2.2.1. Equations of velocity.

The first finite-difference approximation is obtained by central-difference formula :-

$$\frac{\partial U}{\partial Y}\Big|_{i,j} = \frac{U_{i,j+1} - U_{i,j-1}}{2\Delta Y} \quad (8)$$

For the second order derivative, the central-difference approximation is given by,

$$\frac{\partial^2 U}{\partial Y^2}\Big|_{i,j} = \frac{U_{i,j+1} - 2U_{i,j} + U_{i,j-1}}{2\Delta Y^2} \quad (9)$$

The backward-difference approximation in the X-direction is

$$\frac{\partial U}{\partial X}\Big|_{i,j} = \frac{U_{i,j} - U_{i-1,j}}{\Delta X} \quad (10)$$

$$U \frac{\partial U}{\partial X}\Big|_{i,j} = U_{i-1,j} \frac{U_{i,j} - U_{i-1,j}}{\Delta X} \quad (11)$$

$$V \frac{\partial U}{\partial Y}\Big|_{i,j} = V_{i-1,j} \frac{U_{i,j+1} - U_{i,j-1}}{2\Delta Y} \quad (12)$$

By substituting in the momentum equation:

$$\left[-\frac{V_{i-1,j}}{2\Delta Y} - \frac{1}{\Delta Y^2}\right] U_{i,j-1} + \left[\frac{U_{i-1,j}}{\Delta X} + \frac{2}{\Delta Y^2}\right] U_{i,j} + \left[\frac{V_{i-1,j}}{2\Delta Y} - \frac{1}{\Delta Y^2}\right] U_{i,j+1} = \theta_{i-1,j} \beta^* + \frac{U_{i-1,j}^2}{\Delta X} \quad (13)$$

2.2.2. Energy equation

$$U \frac{\partial \theta}{\partial X}\Big|_{i,j} = U_{i-1,j} \frac{\theta_{i,j} - \theta_{i-1,j}}{\Delta X} \quad (14)$$

$$V \frac{\partial \theta}{\partial Y} \Big|_{i,j} = V_{i-1,j} \frac{\theta_{i,j+1} - \theta_{i,j-1}}{2\Delta Y} \quad (15)$$

$$\frac{\partial^2 \theta}{\partial Y^2} \Big|_{i,j} = \frac{\theta_{i,j+1} - 2\theta_{i,j} + \theta_{i,j-1}}{\Delta Y^2} \quad (16)$$

By replacing into the energy equation yields:

$$\left[-\frac{V_{i-1,j}}{2\Delta Y} - \frac{1}{Pr\Delta Y^2} \right] \theta_{i,j-1} + \left[\frac{U_{i-1,j}}{\Delta X} + \frac{2}{Pr\Delta Y^2} \right] \theta_{i,j} + \left[\frac{V_{i-1,j}}{2\Delta Y} - \frac{1}{Pr\Delta Y^2} \right] \theta_{i,j+1} = \frac{U_{i-1,j} \theta_{i-1,j}}{\Delta X} \quad (17)$$

2.2.3. Continuity equation

For continuity equation the derivatives are discretized at the midpoint ($i,j - 0.5$).

$$\frac{\partial V}{\partial Y} \Big|_{i,j-0.5} = \frac{V_{i,j} - V_{i,j-1}}{\Delta Y} \quad (18)$$

$$\left[\frac{\partial U}{\partial X} \right]_{i,j-0.5} = \frac{1}{2} \left[\left(\frac{\partial U}{\partial X} \right)_{i,j} + \left(\frac{\partial U}{\partial X} \right)_{i,j-1} \right] \quad (19)$$

$$\frac{\partial V}{\partial Y} = -\frac{\partial U}{\partial X} \quad (20)$$

$$V_{i,j} = V_{i,j-1} - \left(\frac{\Delta Y}{2\Delta X} \right) (U_{i,j} - U_{i-1,j} + U_{i,j-1} - U_{i-1,j-1}) \quad (21)$$

2.3. Heat-Transfer Coefficient

The numerical calculation of the heat-transfer coefficient is:-

$$h_x = -\frac{k}{(T_w - T_\infty)} \left(\frac{\partial T}{\partial y} \right)_{y \rightarrow 0} \quad (22)$$

Where the derivative is calculated numerically by taking the first row of temperature in numerical solution:-

$$\left(\frac{\partial T}{\partial y} \right)_{y \rightarrow 0} \cong \frac{T_{(i,2)} - T_w}{\Delta y} \quad (23)$$

For Nusselt Number:-

$$Nu_x = \frac{h_x x}{k} \quad (24)$$

For Rayleigh Number:-

$$Ra_x = \frac{\beta_{ref} g (T_w - T_\infty) x^3}{\gamma \alpha} \quad (25)$$

$$\text{Where } \beta_{ref} = \frac{1}{T_f} \quad \text{and } T_f = \frac{1}{T_w + T_\infty} \quad (26)$$

2.4. Equation-of-State Approach

The equations of state derived from van der Waals, [10] presented a general form for cubic equations of state suitable at high pressures and temperatures suitable for supercritical fluids:

$$P = \frac{RT}{V' - b} - \frac{a}{V'^2 + u'bV' + wb^2} \quad (27)$$

where a and b are constants, obtained from the critical properties.

2.5. Thermal Expansivity

The definition of isobaric thermal expansivity β :

$$\beta = \frac{1}{T} \left[1 - \left(\frac{Z^2 B - 2ZA + 3AB}{3Z^3 - 2Z^2(B+1) + ZA} \right) \right] \quad (28)$$

Where

$$Z = \frac{PV'}{RT}, \quad A = \frac{aP}{(RT)^2}, \quad B = \frac{bP}{RT} \quad (29)$$

3. Results and Discussion

The above mentioned equations were solved numerically by finite differences. A FORTRAN code was improved to obtain the velocity and temperature profiles along the plate. Figure .5 presents results of (β) calculated by the thermodynamic model, based on the Van der Waals, EOS (28) for refrigerants R134a, R1234yf, R404a. The equation depicted an excellent representation of the data. These values are represented graphically for different values of Pr , Tr for (1.05, 1.1, 1.2, 1.4 and 1.6). The first value (Pr , $Tr = 1.05$) which near the critical value shows the developing of the (β) value clearly at the supercritical point that the value increases sharply.

Also the important is the fact that (β) diverges at the critical point. It is clear that pressure for liquids at low (atmospheric) pressure increases with temperature, while for low-pressure gases the opposite is true. Higher-pressure isobars show a liquid-like behavior at lower (subcritical) temperatures, At higher temperatures, the isobars approach the ideal-gas behavior this confirmed by [8].

Figure .6 depicted the expansivity developing for each refrigerant, from the curve trend the fluid R134a showed the higher values for (β) at a fixed value of temperature then refrigerant R1234yf and the last one R404a. The local Nusselt number was then calculated and plotted as a function of the local Rayleigh number. Figure. 7 presented variation of local Nusselt number for refrigerants R134a, R1234yf and R404a. It is observed in these plots that a curve obtained with temperature and pressure far from the critical region approaches. It was also observed that the curves corresponding to supercritical conditions showed high Nusselt number, which means

that the heat transfer considerably increases in the critical region. For a specific value of Rayleigh number the value of Nusselt number increases as the reduced pressure near the critical pressure.

Figures for R134a, R1234yf, R404a show that the line of reduced pressure of 1.05 and 1.1 at almost superimposed. From this case, it can conclude that the effect of the pressure is not significant, while on the other condition when the reduced pressure at 0.2 the line become closer to empirical correlation line. The curve corresponds to the empirical correlation is obtained from relation that was proposed by Churchill and Chu (1975)[12]

$$Nu = 0.68 + \frac{0.67Ra^{0.25}}{[(1 + \frac{0.492}{Pr})^9 / 16]^{1/4} / 9} \quad 0 < Ra < 10^9 \quad (30)$$

Figure .8 depicts the boundary layer for variable values of reduced pressures. The graphs showed that there is a thinner velocity profile at reduced pressure near the critical value. Figure.9 depicts the variation of temperature along y-direction at the same conditions of figure.8 that depict the velocity variations. The graphs showed that the temperature increases as the reduced pressure increases. Figure. 10 (a) showed the velocity contour lines for R134a at Pr =1.05 , each line represents the velocity values at the hydrodynamic boundary layer. For the same values of contour lines, figure.10 (b) showed the temperature contour lines with the temperature values for the thermal boundary layer.

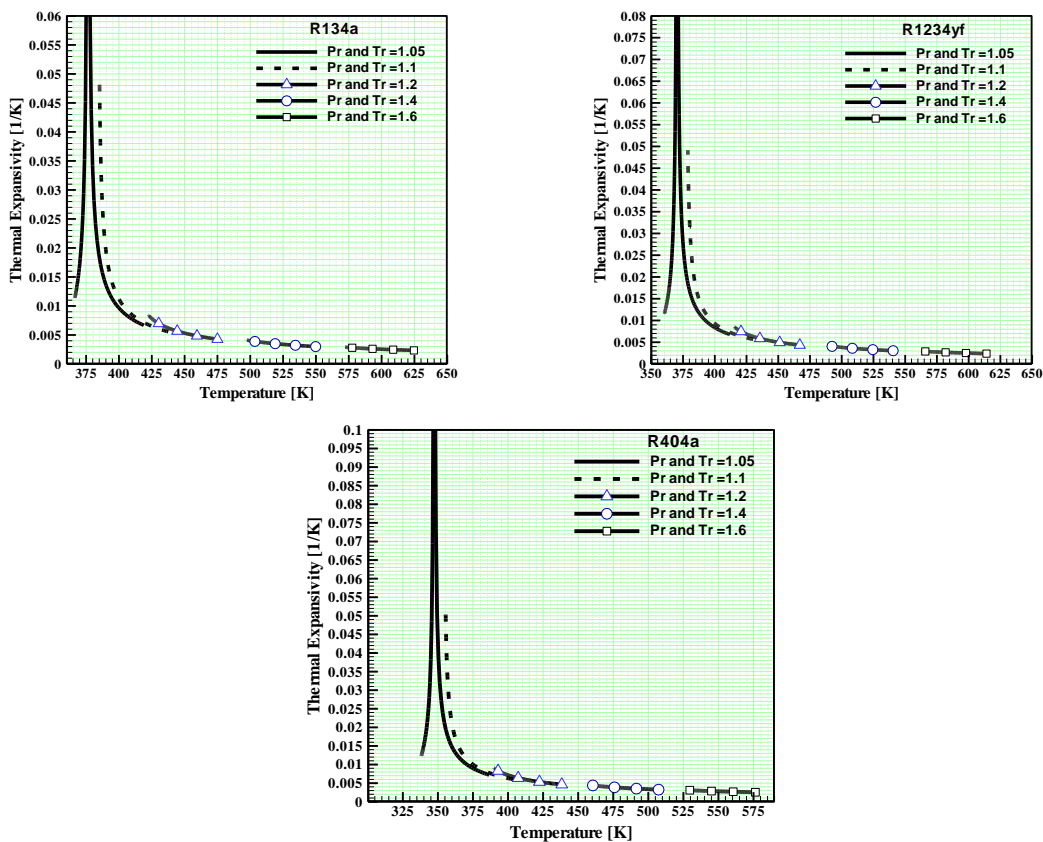


Figure 5. Thermal expansivity for refrigerants at different reduced pressure.

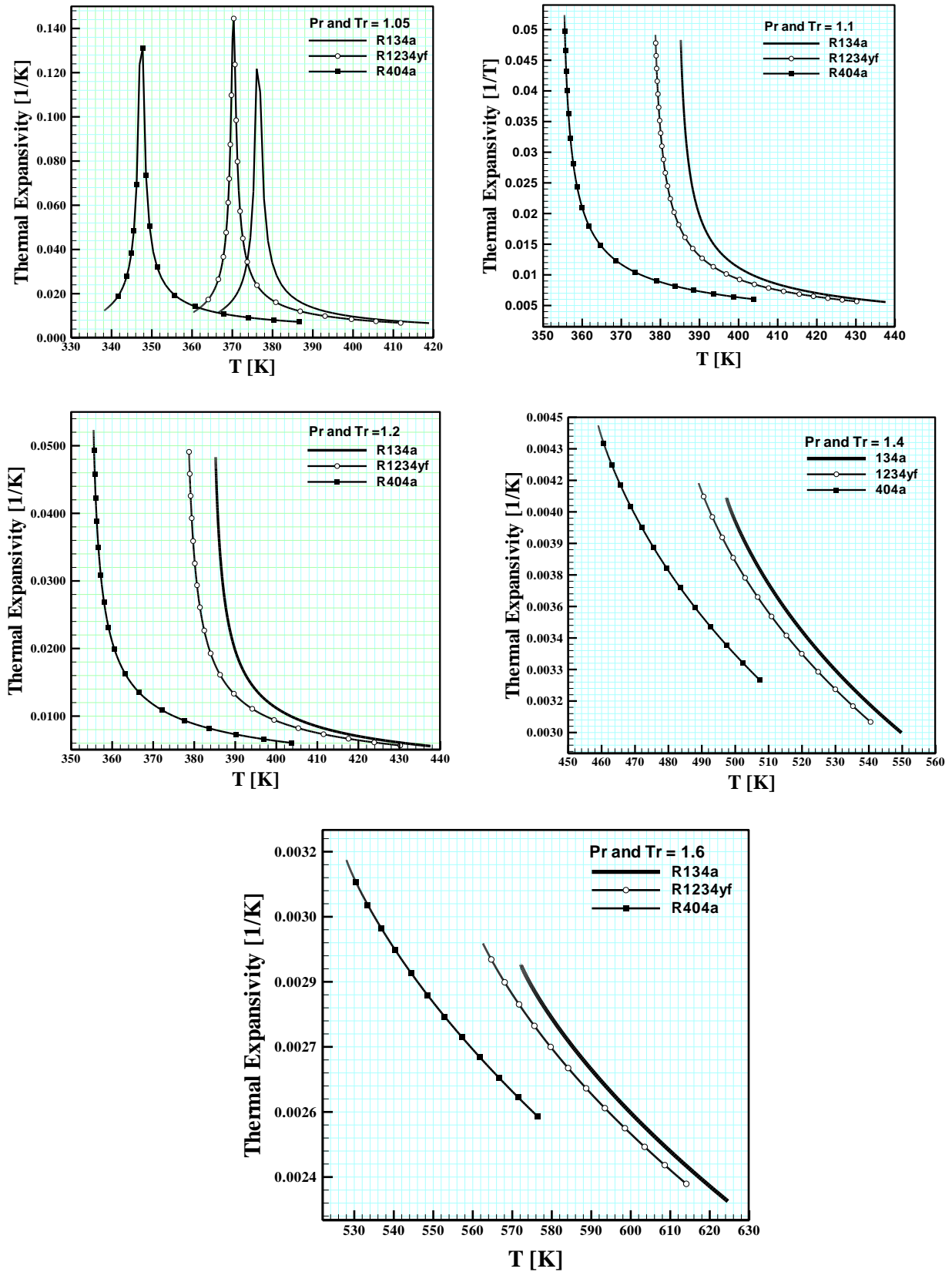


Figure 6. Thermal expansivity for refrigerants at different reduced pressures

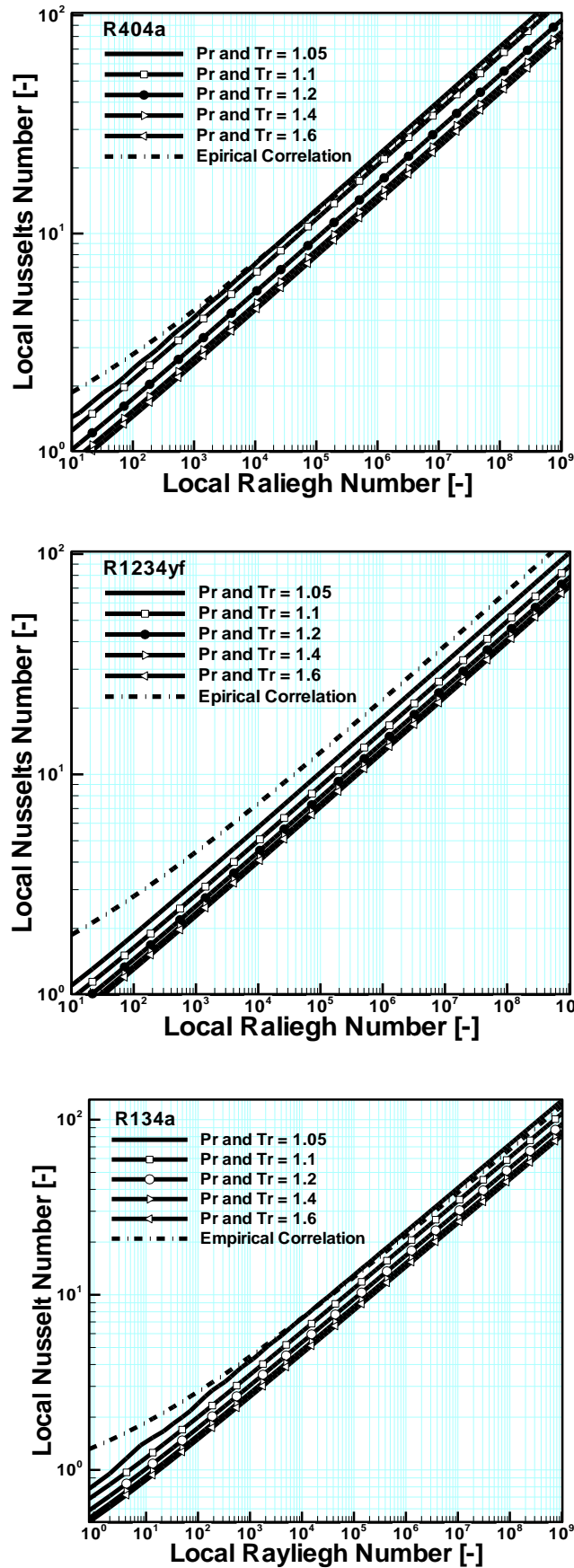


Figure 7. Nusselt Number as a function of Rayleigh Number.

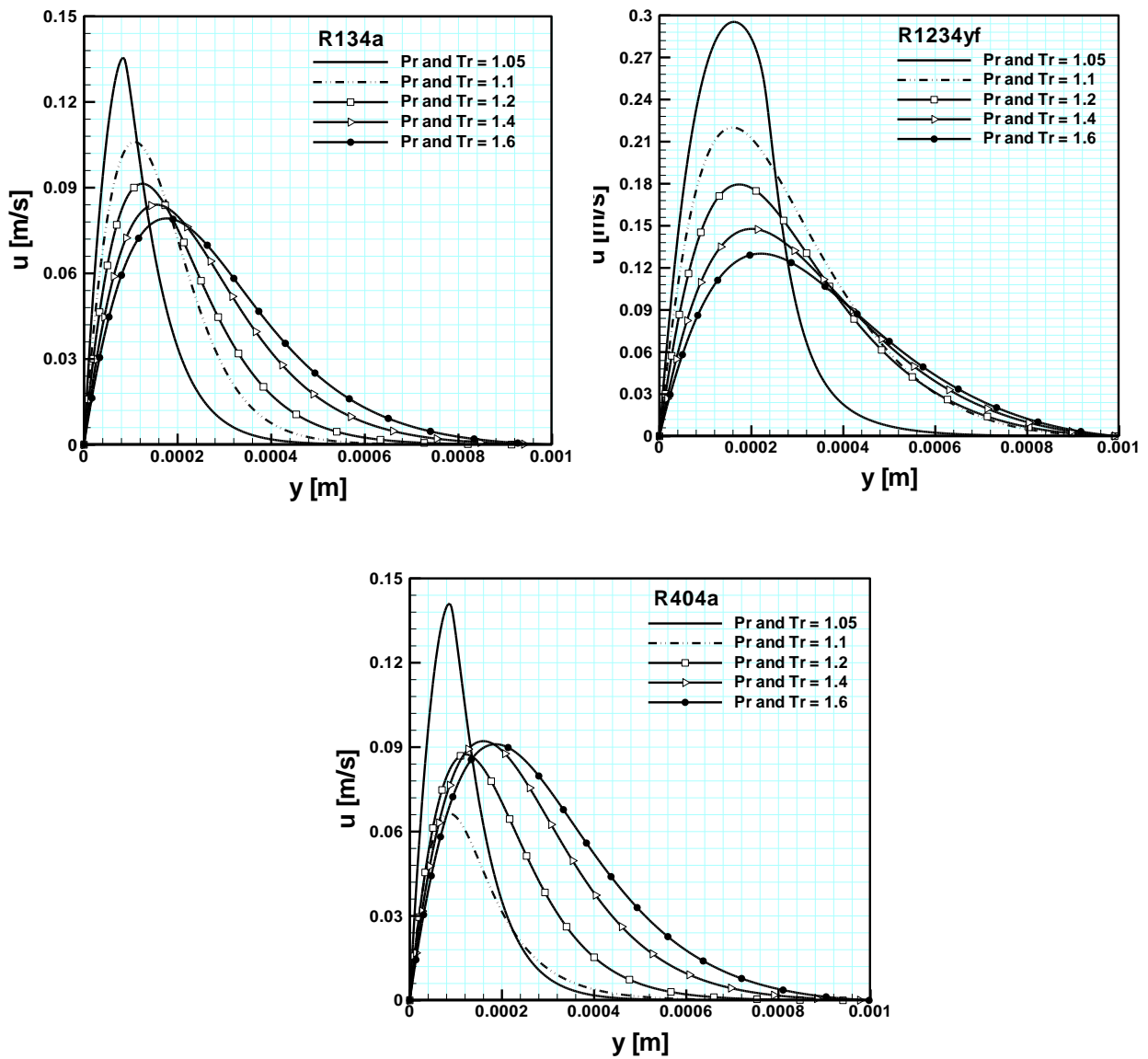


Figure 8. Dimensional velocity profile at different reduced pressure

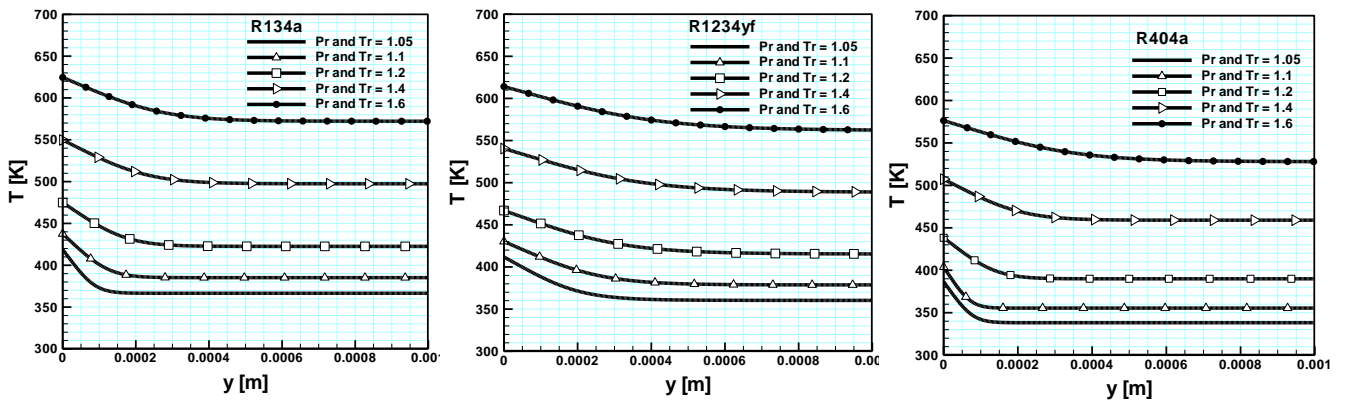


Figure 9. Temperature variation at different reduced pressure and temperature

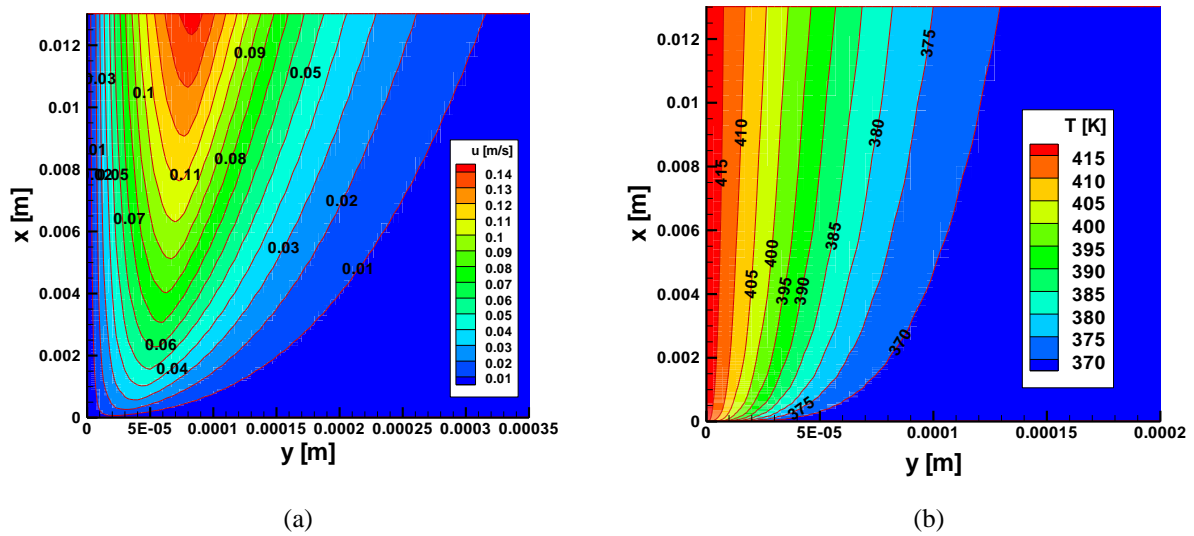


Figure 10. Velocity and temperature contour lines for R134a at Pr and Tr = 1.05

4. Conclusions

In the present work vertical flat plate was used as a geometry to study the behaviour of the hydrofluorocarbons in natural convection under supercritical conditions at uniform heat flux.

1. It has being shown that the Van dre Waals (EOS) giving reasonable approach in calculating the thermo-physical properties of supercritical Hydrofluorocarbons
2. The thermal expansivity has a varies considerably with reduced pressures and reduced temperatures although the behavior near critical point (Pr and Tr = 1.05, 1.1) showed sharp variation.
3. The values of Nusselt number with variation of Raleigh number decreases as the reduced pressure and reduced temperature increases, and the classic correlation that was proposed by Churchill and Chu (1975) works well in the critical zone.
4. The dimensional velocity and temperature along the vertical plate was plotted. The contour lines draw the thermal and hydrodynamic boundary layer and explained the fluid behavior above supercritical conditions.

5. Nomenclatures

a	EOS constant that corrects for intermolecular attractive forces, $[\text{N} \cdot \text{m}^4 / \text{mol}^2]$
A	Dimensionless EOS parameter, [-]
b	EOS constant that corrects for volume of gas molecules, $[\text{m}^3 / \text{mol}]$
B	Dimensionless EOS parameter, [-]
Gr	Grashof number [-]
P_c	Critical pressure [Pa]
P	Pressure [Pa]
P_r	Prandtl number, [-]

Pr	Reduced pressure P/P_c , [-]
x	Coordinate parallel to the vertical plate, [m]
X	Dimensionless coordinate parallel to the vertical plate, [-]
T	Temperature [K]
T_c	Critical temperature [K]
Tr	Reduced temperature T/T_c , [-]
u	Velocity component in the x direction, [m/s]
U	Dimensionless velocity component in the x direction, [-]
u'	EOS parameter, [-]
v	Velocity component in the y direction, [m/s]
V	Dimensionless velocity component in the y direction, [-]
V'	Molar volume, [m ³ /mol]
W	Domain width [m]
Z	Compressibility factor, [-]

Greek symbols

γ	Kinematic viscosity, [m ² /s]
θ	Dimensionless temperature, [-]
β	Thermal expansion coefficient (thermal expansivity), [1/K]
β_{ref}	Reference value of the thermal expansivity, [1/K]
β^*	Dimensionless thermal expansivity, [-]

Subscript

c	Critical
i	Node in the direction
j	Node in they direction
ref	Reference
s	Surface
∞	Outside the boundary layer

Abbreviations

EOS	Equations of state
-----	--------------------

6. References

1. Ali J. Chamkha , Camille Issa , Khalil Khanafer , 2002 “*Natural convection from an inclined plate embedded in a variable porosity porous medium due to solar radiation*,” *Int. J. Therm. Sci.* 41, 73–81
2. Luca Barbazza , Leonardo Pierobon , Alberto Mirandola and Fredrik Haglind, (2014) “*Optimal Design Of Compact Organic Rankine Cycle Units For Domestic Solar Applications*,” *THERMAL SCIENCE*:, Vol. 18, No. 3, pp. 811-822,.
3. Chen-Ru Zhao, Pei-Xue Jiang , (2011) “*Experimental study of in-tube cooling heat transfer and pressure drop characteristics of R134a at supercritical pressures* “ , *Experimental Thermal and Fluid Science* 35, 1293–1303.
4. Calm, J.M., 2008 , “*The next generation of refrigerants – Historical review, considerations, and outlook*,” . *International Journal of Refrigeration*,. 31(7): p.1123-1133.

5. Anusha.Peyyala and N.V.V.S.Sudheer , 2016 “*Possibility of Using Refrigerant Blends In the Existing Refrigerator & AC Systems: A Review*, “ IOSR Journal of Mechanical and Civil Engineering (IOSR-JMCE) e-ISSN: pp. 2278-1684, -ISSN: 2320-334X, Volume 13, Issue 3 Ver. V (May- Jun. 2016), PP 63-70.
6. KOUSAR Nabeela and LIAO ShiJun, (2010). “ *Series solution of non-similarity natural convection boundary-layer flows over permeable vertical surface*“, SCIENCE CHINA Physics, Mechanics and Astronomy, February 2010 Vol. 53 No. 2: 360–368.
7. Ostrach, S. (1952). “*An analysis of laminar free-convection flow and heat transfer about a flat plate parallel to the direction of the generating body force*”. Technical Report 2635,NACA,Washington.
8. Ali Reza Teymourtasha, Danyal Rezaei Khonakdara, Mohammad Reza Raveshib, 2013“*Natural convection on a vertical plate with variable heat flux in supercritical fluids*“, Journal of Supercritical Fluids 74,115– 127.
9. Fayadh M. Abed and Dr. Ghazi Y. M. Alshahery , (2010). “*Model Treatment for Simulation of Natural Convection in A vertical Wall Immersed In a Supercritical Fluid*“, International Journal of Chemical Engineering and Applications, Vol. 1, No.1, June , ISSN: 2010-0221.
10. Schmidt, G., Wenzel, H., 1980. “*A modified van der Waals type equation of state*”. Chem. Eng. Sci. 35, 1503–1512.
11. Rolando C. 2004. “*Natural Convection in Super critical Fluids*”. M.Sc. thesis ,University of Puerto Rico, Greece.
12. Churchill, S. W. and H. H. S. Chu; 1975; “*Correlation Equations for Laminar and Turbulent Free Convection from a Vertical Plate*,”. Int. J. Heat Mass Transfer, 18, 1323.